# CHAPTER VII

# CORRELATIONS

In this chapter we continue our examination of the experimental results looking at correlations between area (or radius) and number of sides, "Lewis' Law," and correlation's between the number of sides of neighboring bubbles, the Aboav-Weaire relation.

## VII.a "Lewis' Law"

Of the aggregate quantities derivable from the area distribution functions, the average area of an $n$-sided bubble as a function of $n$ is the most robust diagnostic. The relationship had been evaluated by Fradkov, Shvindlerman, and Udler, Beenakker, Marder, and others.[27,28,76,77,157] The most commonly assumed relation is that of Lewis, originally proposed for the epithelial cells of the cucumber, that the area of a polygonal cell should be a linear function of its number of sides,[141] i.e.,

$$< a_n >= c_1 + c_2 \cdot n \qquad \text{(VII.1)}$$

at any fixed time, where $c_1$ and $c_2$ are fitting parameters.

Glazier, Gross and Stavans have measured this relation by hand for various stages in the evolution of a two dimensional helium froth and Glazier *et al.* from directly digitized images. The hand measured results cover several different times during the helium run indicated in Figs. 16 (d) and 9 (a). The direct digitization results are available for the entire run shown in Fig.

17 and allow us to calculate an ensemble average of different times to improve our statistics. In their hand measurements Glazier, Gross and Stavans estimated areas by connecting the vertices and centers of sides of bubbles by straight lines and measuring the area of the resulting polygon using a digitizing tablet. Since the walls of few-sided bubbles are convex and the walls of many-sided bubbles concave, this method caused them to systematically underestimate the area of few-sided bubbles and overestimate the area of many-sided bubbles by up to a few percent. Glazier *et al.* measured areas directly by counting pixels and should thus have achieved better accuracy.

We present experimental measurements of normalized bubble areas (i.e. $\lambda_n \equiv \frac{<a_n>}{<a>}$) as a function of $n$ in Fig. 43 for the hand measured data and in Fig. 44 for Glazier *et al.*'s directly digitized data along with their results of the Potts model simulation starting with identical initial conditions on the next nearest neighbor square lattice. Beginning with random initial conditions on the nearest neighbor hexagonal lattice gave identical results. We observe that the area for few-sided ($n = 3, 4$) bubbles is larger than that predicted by Lewis' hypothesis, in agreement with the models of Fradkov, Shvindlerman and Udler, Beenakker, Marder, and Weaire and Kermode, but disagreeing with the predictions of Rivier.[198] Lewis' Law is seen to work poorly for few-sided bubbles. Indeed, for many runs, a linear fit actually predicts negative areas for three- and four-sided bubbles. Many-sided ($n > 8$) bubbles are smaller than predicted as well, though this discrepancy may be due to memory of the initial length scale. The correlation seems to be

independent of the degree of equilibration of the froth and the distributions of normalized area are constant to within experimental error (typically 5%) at all times, suggesting that they depend on local rather than long range equilibration. For example, a very large few-sided bubble can rapidly shed sides by $T1$ processes without having to wait for bubbles to disappear.

In Table 9 we present side-area correlations for a few models and experimental systems. We normalize $A_6$ to one, which is not ideal (we would prefer to look at $\lambda_n$) but is at least consistent and does not require us to know $< a >$ for all categories. We can easily distinguish the biological patterns which obey Lewis' law from the coarsening patterns which do not. The correlations for the soap froth and two dimensional grain growth in aluminum are comparable for large $n$. For small $n$, the grains are much larger than the bubbles, suggesting a mechanism stabilizing small few-sided grains in the metal. Of the models, the Potts model gives almost identical results to the froth. The vertex model of Nakashima *et al.* also does well. The mean field theories all tend to have both few- and many-sided bubbles too large, again suggesting a failure to consider an anticorrelation in side redistribution. Large few-sided bubbles are less likely to lose sides than small few-sided and large many-sided bubbles, and thus there are fewer large few-sided bubbles produced than predicted by the uncorrelated mean field theories. As we might expect neither the Voronoi construction nor the first model of Almeida and Iglesias are within range. The second model of Almeida and Iglesias does better but is still too weakly correlated.

**Fig. 43 Lewis' Law.** Normalized average area of an $n$-sided bubble versus $n$ for a two dimensional helium froth at four different times during a run. (a) $t = 2.52$ hours. (b) $t = 8.63$ hours. (c) $t = 12.45$ hours. (d) $t = 64.32$ hours. To within experimental error the four correlations are identical (From Glazier, Gross and Stavans 1987).[94]

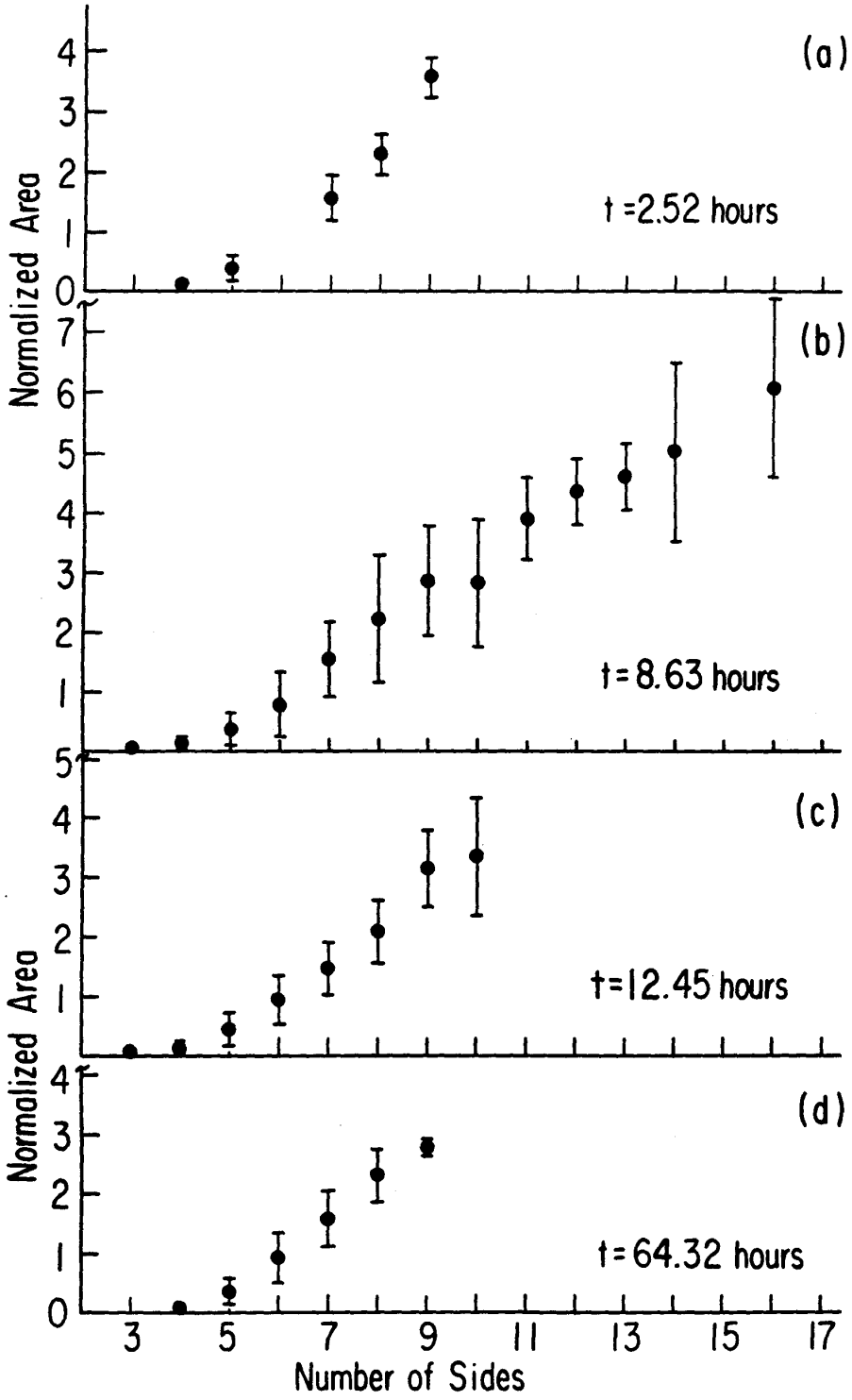
(a)
t =2.52 hours
(b)
t=8.63 hours
(c)
t=12.45 hours
(d)
t=64.32 hours
Normalized Area
Normalized Area
Number of Sides
0
1
2
3
4
5
6
7
3
5
7
9
11
13
15
17

**Fig. 44 Lewis' Law.** Normalized average area of an $n$-sided bubble versus $n$ for a two dimensional air froth (circles), $Q = 48$ hexagonal lattice Potts model (triangles), and $Q = 48$ next nearest neighbor square lattice Potts model (diamonds). To within experimental error the correlations are identical (From Glazier *et al.* 1989).[93]

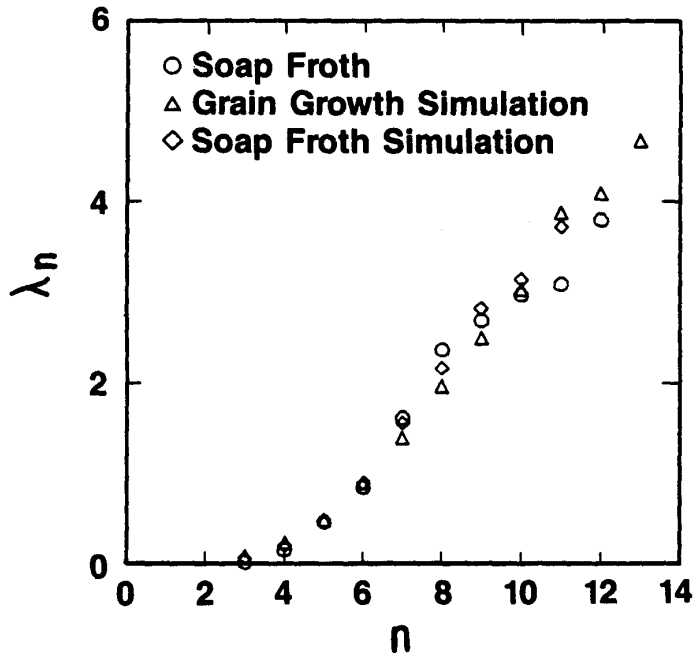
Soap Froth
Grain Growth Simulation
Soap Froth Simulation
λn
n
0
2
4
6
8
10
12
14

**Fig. 45 Radius Law.** Normalized average radius of an $n$-sided bubble versus $n$ for a two dimensional air froth (circles), $Q = 48$ hexagonal lattice Potts model (triangles), and $Q = 48$ next nearest neighbor square lattice Potts model (diamonds). To within experimental error the correlations are identical (From Glazier *et al.* 1989).[93]

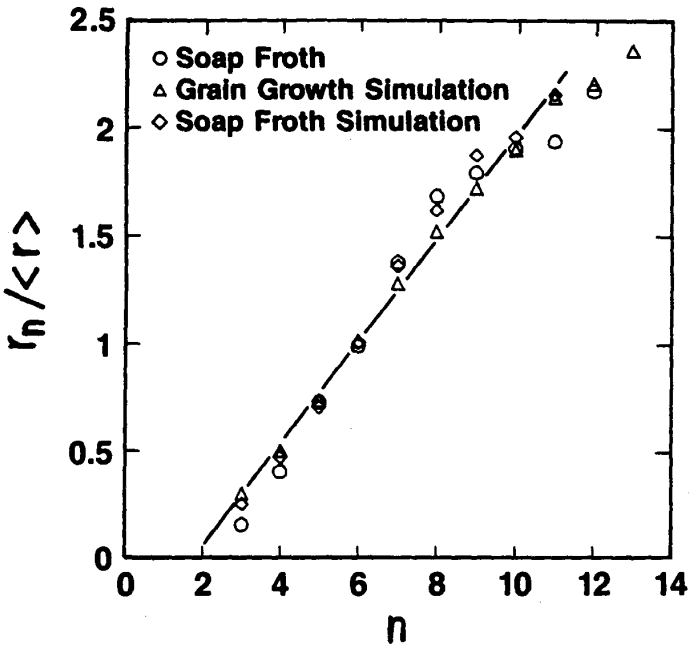
Soap Froth
Grain Growth Simulation
Soap Froth Simulation
$r_n/\langle r\rangle$
n
0
0.5
1
1.5
2
2.5
0
2
4
6
8
10
12
14

## TABLE 9

## LEWIS' LAW

| System | $A_3$ [$A_2$] | $A_4$ | $A_5$ | $A_6$ ($A_{11}$) | $A_7$ ($A_{12}$) | $A_8$ ($A_{13}$) | $A_9$ ($A_{14}$) | $A_{10}$ ($A_{15}$) |
|---|---|---|---|---|---|---|---|---|
| **Experiment** | | | | | | | | |
| Soap Froths | | | | | | | | |
| Averaged Air[95] | 0.04 | 0.18 | 0.56 | 1.00 (4.61) | 1.96 | 2.84 | 3.19 | 3.75 |
| Averaged Helium | 0.05 | 0.17 | 0.44 | 1.00 (4.61) | 1.73 | 2.38 | 2.96 | |
| Metal Grains | | | | | | | | |
| Al Foil[75] | 0.12 [0.16] | 0.37 | 0.56 | 1.00 (4.35) | 1.41 (5.15) | 2.12 | 3.25 | 3.55 |
| Biological[142] | | | | | | | | |
| Cucumber 100mm | – | 0.51 | 0.76 | 1.00 | 1.29 | 1.49 | 1.60 | |
| Cucumber 200mm | – | 0.52 | 0.78 | 1.00 | 1.21 | 1.44 | 1.64 | |
| Amnion | 0.42 | 0.59 | 0.82 | 1.00 | 1.20 | 1.35 | 1.59 | |
| Other Materials | | | | | | | | |
| Agfa Film[142] | 0.08 | 0.20 | 0.46 | 1.00 | 1.68 | 2.43 | 3.49 | 4.49 |
| **Theory** | | | | | | | | |
| Weaire[244] | – | 0.12 | 0.38 | 1.00 | 1.39 | 1.87 | 2.87 | 3.17 |
| Almeida & Iglesias (I)[10] | 0.66 | 0.85 | 0.94 | 1.00 | 1.02 | 1.05 | 1.06 | 1.07 |
| Almeida & Iglesias (II)[11] | 0.17 | 0.36 | 0.63 | 1.00 (3.60) | 1.40 (4.29) | 1.89 | 2.40 | 2.99 |
| Marder[157] | 0.24 | 0.35 | 0.56 | 1.00 (3.18) | 1.53 (3.60) | 2.04 | 2.49 | 2.93 |
| Fradkov *et al.*[76] | 0.53 | 0.53 | 0.71 | 1.00 (6.47) | 1.96 (7.71) | 2.80 | 3.95 | 4.91 |
| Beenakker[26] | 0.38 | 0.46 | 0.62 | 1.00 (5.35) | 1.75 | 2.63 | 3.49 | 4.39 |
| Voronoi[82] | 0.51 | 0.66 | 0.82 | 1.00 | 1.17 | 1.35 | 1.55 | 1.67 |
| Potts Model[98] | 0.03 | 0.23 | 0.53 | 1.00 (4.37) | 1.83 (4.70) | 2.35 (–) | 3.07 (5.37) | 3.53 |
| Nakashima *et al.*[179] | 0.002 | 0.17 | 0.45 | 1.00 (4.36) | 1.72 (5.13) | 2.39 | 3.06 | 3.64 |

## TABLE 10

## RADIUS LAW

| System | $r_3$ | $r_4$ | $r_5$ | $r_6$ ($r_{11}$) | $r_7$ ($r_{12}$) | $r_8$ ($r_{13}$) | $r_9$ ($r_{14}$) | $r_{10}$ ($r_{17}$) |
|---|---|---|---|---|---|---|---|---|
| **Experiment** | | | | | | | | |
| **Two Dimensional Growth** | | | | | | | | |
| Air Froth[93] | 0.15 | 0.40 | 0.73 | 1.00 (1.96) | 1.40 (2.21) | 1.71 | 1.82 | 1.93 |
| Al Foil[75] | – | 0.48 | 0.72 | 1.00 (2.23) | 1.13 (2.52) | 1.58 (–) | 1.93 (2.76) | 2.10 |
| **Two Dimensional Sections of Three Dimensional Grain Growth** | | | | | | | | |
| Tin[64] | 0.26 | 0.49 | 0.69 | 1.00 (2.83) | 1.23 (2.91) | 1.63 (3.31) | 1.83 (3.23) | 2.37 (3.49) |
| MgO + LiF[9] | 0.25 | 0.47 | 0.72 | 1.00 (2.23) | 1.27 (2.45) | 1.53 | 1.73 | 1.96 |
| **Theory** | | | | | | | | |
| Topological[76] | 0.57 | 0.61 | 0.76 | 1.00 (2.21) | 1.38 | 1.67 | 1.96 | 2.13 |
| Vertex Model[179] | 0.15 | 0.36 | 0.64 | 1.00 (2.40) | 1.56 | 1.76 | 1.93 | 2.15 |
| Vertex[62] | 0.16 | 0.27 | 0.64 | 1.00 | 1.34 | 1.59 | 1.66 | |
| Topological[28] | 0.62 | 0.66 | 0.77 | 1.00 | 1.37 | 1.70 | 1.99 | 2.23 |
| Potts Model[250] | 0.27 | 0.49 | 0.73 | 1.00 (2.17) | 1.34 (2.22) | 1.60 (2.39) | 1.82 | 1.95 |

If we plot instead $r_n \equiv \frac{<a_n>^{.5}}{<a>^{.5}}$ the graph is significantly more linear, with just a hint of $S$-curve rollover for large $n$. We show Glazier *et al.*'s result for an air froth in Fig. 45. In this case because of the scarcity of many-sided bubbles we may well be observing a subtle selection effect: large many-sided bubbles are more likely to intersect the frame boundary than small bubbles and are hence more likely to be excluded from consideration, resulting in a lower apparent size for large $n$. Once again we find that the soap froth, the hexagonal lattice Potts model and the next nearest neighbor square lattice Potts model give essentially identical results.

We have fewer examples where radius correlations are quoted than we have area correlations. We summarize the available data in Table 10. Once again we have used the normalization, $r_6 = 1$. The agreement between the soap froth and the aluminum foil is reasonable, though the foil has slightly larger many-sided grains. Surprisingly, the two dimensional sections of three dimensional grains give results essentially indistinguishable from true two dimensional coarsening. As we would expect, the Potts model and the vertex model of Nakashima *et al.* give the best agreement with experiment. The uncorrelated mean field theories predict excessively large few-sided bubbles. In all cases the overall linearity of the correlation is good, and the radius law

$$< r_n >= c_1 + c_2 \cdot n \qquad \text{(VII.2)}$$

seems verified for both two and three dimensional grain growth, at least for $n$ small enough that we are able to obtain reasonable statistics.

Our conclusion is twofold. First: the radius law seems to work for grain

growth while Lewis' law fails (though the latter works for biological aggregates with constrained area distributions). Second: all of the models that seem physically reasonable give good agreement with experiment, the models that we think of as coming closest to the actual physics, like the Potts model giving the best results. The agreement also provides added evidence for the existence of an anticorrelation in side redistribution, which is apparent in the mean field theory's predictions of larger size few-sided bubbles.

### VII.b Aboav-Weaire Law

The simplest side correlation function to measure (and the only one that can be reliably calculated given the available statistics) is the average number of sides of the neighbors of an $n$-sided bubble, $m(n)$. Assuming statistical equilibrium and short range interactions, Rivier and Weaire have both provided arguments for the form of this function.[134,135,199,236]

Rivier's argument is particularly elegant. In this case $nm(n)$ is the average total number of sides of the neighbors of an $n$-sided bubble. Consider a bubble with $n$ sides next to a three-sided bubble, and the two common neighbors, $a$ and $b$. Then

$$nm(n) = n_a + n_b + 3 + n_{other}, \tag{VII.3}$$

where $n_{other}$ is the number of sides of the remaining grains adjacent to the bubble. If the three-sided bubble disappears, the original bubble and its neighbors each lose a side, and the total number of sides of the remaining

neighbors decreases by 2, so

$$(n-1)m(n-1) = n_a + n_b - 2 + n_{other}. \tag{VII.4}$$

Assuming that $m(n)$ is unchanged by the disappearance as it must be in a scaling state yields a recursion relation

$$(n-1)m(n-1) + 5 = nm(n), \tag{VII.5}$$

which is solved by

$$m(n) = 5 + \frac{c}{n}, \tag{VII.6}$$

where $c$ is an arbitrary constant.

We may argue even more simply as follows. Assume that there are no long range correlations or stresses in the lattice. Then topological charge (which represents residual stress) should be locally screened. Consider an $n$-sided bubble. Its topological charge is $\mathcal{T} = n-6$. Therefore nearest neighbor charge screening requires that the bubble's nearest neighbors must have a total topological charge of $\mathcal{T} = 6-n$. Thus the average topological charge of each neighbor is $\mathcal{T} = \frac{6-n}{n}$, so

$$m(n) = 6 - \frac{6-n}{6} = 5 + \frac{6}{n}. \tag{VII.7}$$

A longer range interaction with weak local correlation will change the constants, but we expect a general form:

$$m(n) = \kappa_1 + \frac{c}{n}. \tag{VII.8}$$

Weaire has argued on physical grounds that the correct form of the relation is

$$m(n) = 6 - a + \frac{6a + \mu_2}{n}, \qquad \text{(VII.9)}$$

where $\mu_2$ is the second moment of the side distribution and $a$ is a constant of order one.[134,135] This relation is known as the **Aboav-Weaire Law.**

In Fig. 46 we present experimental results for $nm(n)$, measured by Stavans and Glazier for a scaling state of a two dimensional helium froth. They found excellent agreement with the Aboav-Weaire law with the second moment of the distribution $\mu_2 = 1.4$ and $a = 1$. Aboav also obtained good agreement for soap froth patterns with $\mu_2$ ranging from 0.24 to 2.86 during the initial transient, using $a = 1.2$. It is reasonable to expect that longer range correlations (i.e. larger values of $a$) would obtain during a transient which retains some residual order. Similar results also obtain in metal films, and two dimensional sections of three dimensional polycrystals. Since the Aboav-Weaire law depends on the ability of the froth to equilibrate stress locally, it is not surprising that it does not apply to either the Voronoi or Johnson-Mehl models. It does apply to almost all the other models we have discussed. We present a summary of Aboav's Law results in Table 11.

Since the Aboav-Weaire law has two fitting parameters, a and $\mu_2$, the best we can hope for is a general agreement in form among the data presented. In Fig. 47 we show Glazier *et al.*'s comparison between $m(n)$ for the

## TABLE 11

## ABOAV's LAW

| System | $m(3)$ ($m(11)$) | $m(4)$ ($m(12)$) | $m(5)$ ($m(13)$) | $m(6)$ | $m(7)$ | $m(8)$ | $m(9)$ | $m(10)$ |
|---|---|---|---|---|---|---|---|---|
| **Experiment** | | | | | | | | |
| Soap Froth | | | | | | | | |
| Aboav[8] | | | | | | | | |
| V/1 | - | - | 6.29 | 6.03 | 5.84 | | | |
| IV/1 | - | 6.68 | 6.33 | 6.09 | 5.91 | 5.76 | | |
| IV/2 | 7.49 | 6.82 | 6.44 | 6.11 | 5.93 | 5.80 | | |
| IV/3 | 7.86 | 6.96 | 6.49 | 6.19 | 5.99 | 5.87 | 5.76 | |
| IV/6 | 7.97 | 7.09 | 6.59 | 6.28 | 6.10 | 5.95 | 5.78 | |
| IV/8 | 8.4 | 7.4 | 6.7 | 6.4 | 6.2 | 6.1 | 6.0 | |
| Glasier *et al.*[93] | 8.13 (5.90) | 7.31 | 6.65 | 6.34 | 6.19 | 6.07 | 6.04 | 5.87 |
| ± | 2.43 (1.85) | 2.09 (-) | 1.58 (-) | 1.55 | 1.55 | 1.72 | 2.11 | 2.01 |
| Grain Growth | | | | | | | | |
| $Al_2O_3$[30] | 8.08 (5.76) | 7.06 | 6.55 | 6.37 | 6.23 | 5.97 | 5.99 | 6.04 |
| ± | 0.34 (0.17) | 0.17 | 0.08 | 0.08 | 0.08 | 0.08 | 0.11 | 0.28 |
| Al Foil[77] | 6.99 6.06 | 6.78 (-) | 6.60 (6.03) | 6.45 | 6.30 | 6.22 | 6.17 | 6.12 |
| ± | 0.13 (0.10) | - (-) | - (0.10) | - | - | - | - | 0.10 |
| Biological | | | | | | | | |
| Cucumber[142] | - | 6.67 | 6.50 | 6.18 | 5.82 | 5.73 | 5.79 | |
| **Theory** | | | | | | | | |
| Network[77] | 7.71 (5.75) | 7.21 (5.80) | 6.69 (5.75) | 6.39 | 6.24 | 6.14 | 5.97 | 5.78 |
| Vertex Model[179] | 8.51 (5.82) | 7.34 | 6.64 | 6.42 | 6.22 6.04 | 6.12 | 5.96 | 5.88 |
| Potts Model[93] | 8.28 (5.82) | 7.23 (5.68) | 6.65 (5.70) | 6.34 (5.63) | 6.19 | 6.07 | 6.04 | 5.87 |
| ± | 2.09 (1.84) | 1.77 (1.75) | 1.58 (1.75) | 1.55 (1.75) | 1.55 | 1.55 | 1.75 | 1.65 |
| Static[34] | | | | | | | | |
| Voronoi | 6.96 | 6.68 | 6.44 | 6.26 | 6.10 | 6.05 | 5.81 | 5.74 |
| Johnson-Mehl | 7.14 | 6.60 | 6.36 | 6.21 | 6.13 | 6.09 | 5.95 | 6.02 |

**Fig. 46 Aboav-Weaire Law.** Correlation between the number of sides of neighboring bubbles. $m(n)$ is the average number of sides of a bubble next to an $n$-sided bubble. The dots are taken from an equilibrated two dimensional helium froth. The dashed line shows the prediction of the Aboav-Weaire law using $a = 1$ and the measured value of $\mu_2 = 1.4$ (From Stavans and Glazier, 1989).[220]

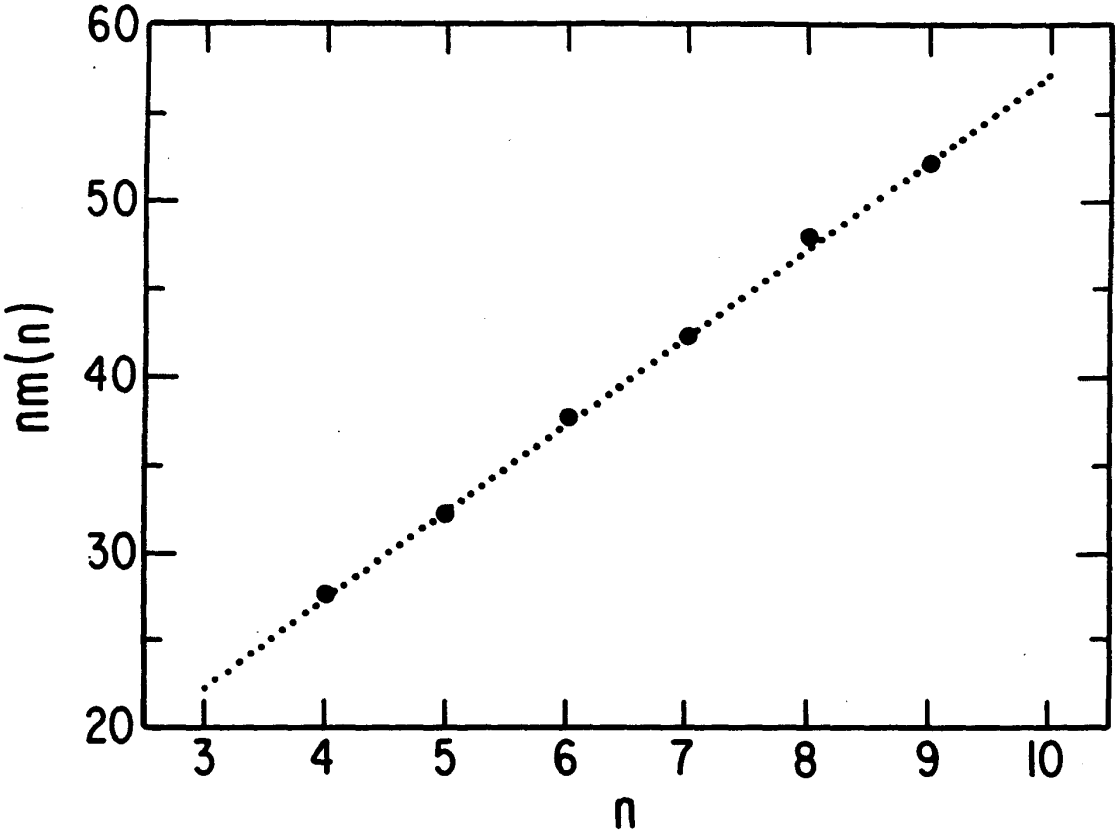
60
50
40
30
20
nm(n)
3
4
5
6
7
8
9
10
n

**Fig. 47 Nearest Neighbor Side Correlations.** Correlation between the number of sides of neighboring bubbles. $m(n)$ is the average number of sides of a bubble next to an $n$-sided bubble. The upper points show the value of $m(n)$, the lower points the standard deviation, for a two dimensional air froth (circles), the $Q = 48$ hexagonal lattice Potts model (triangles), and the $Q = 48$ next nearest neighbor square lattice Potts model (diamonds). To within experimental error the correlations are identical (From Glazier *et al.* 1989).[93]

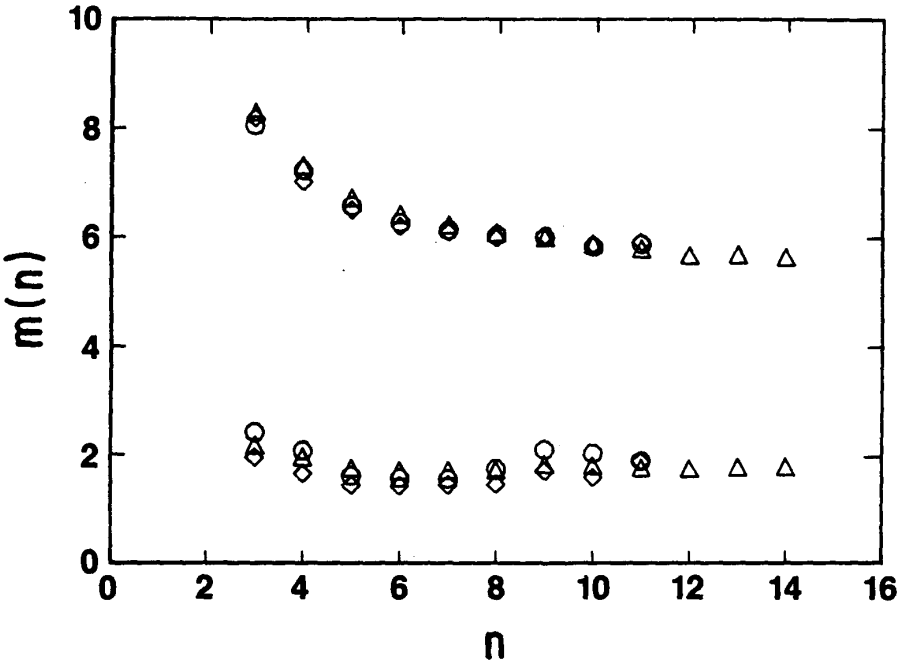
10
8
6
4
2
0
m(n)
0
2
4
6
8
10
12
14
16
n

**Fig. 48 Correlated Side Distributions.** Side distributions of bubbles next to $m$-sided bubbles in the scaling state. Solid lines show distributions for a two dimensional air froth, heavy dashed lines for Potts model. The total distribution function, $\rho(n)$, is given for reference, dotted lines for the air froth and light dashed lines for the Potts model (From Glazier *et al.* 1989).[93]

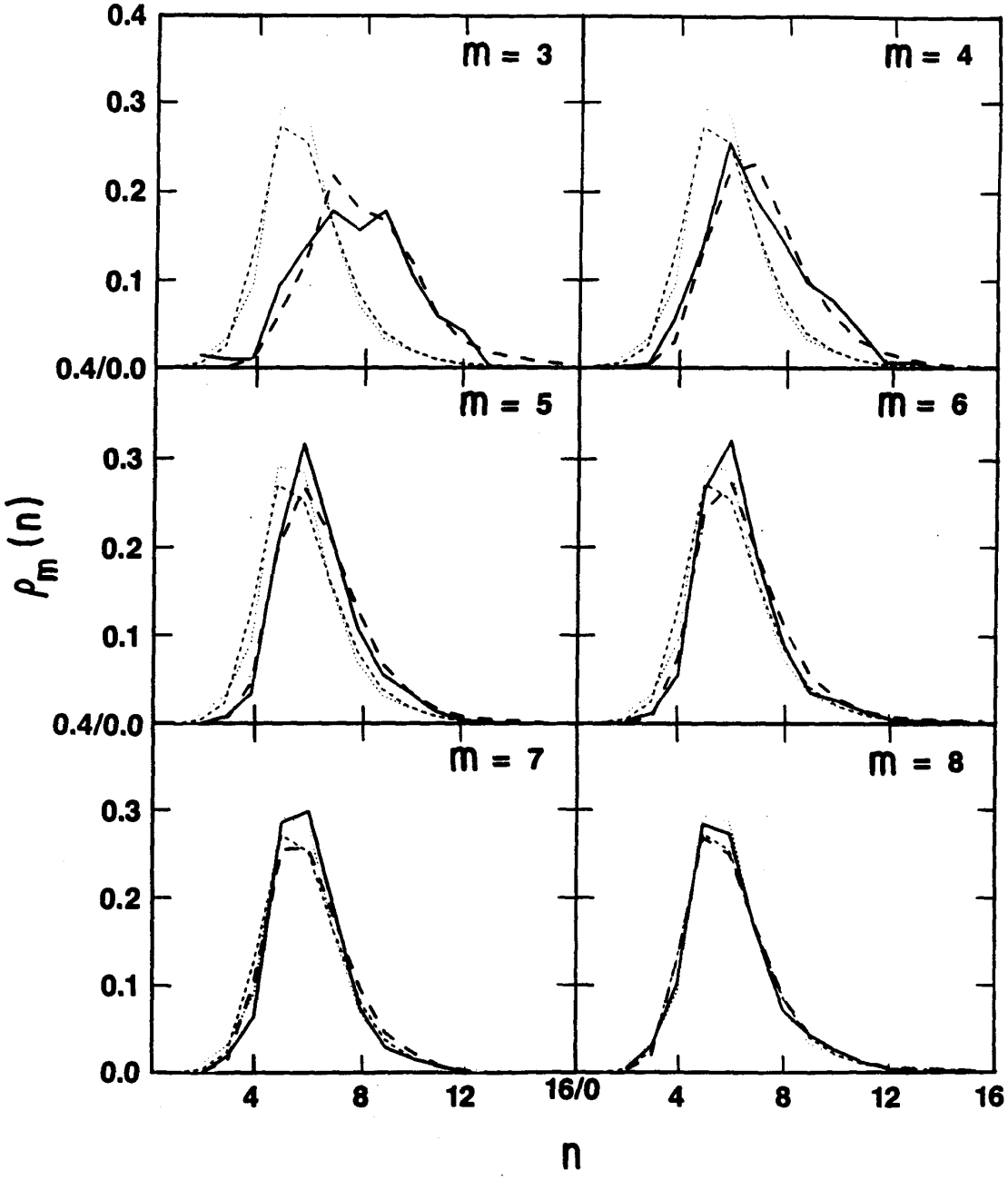
m = 3
m = 4
m = 5
m = 6
m = 7
m = 8
0.4
0.3
0.2
0.1
0.4/0.0
0.0
$\rho_m(n)$
4
8
12
16/0
16
n

soap froth and the Potts model. The results are essentially identical with no free parameters. We can extend the comparison by plotting $\rho_m(n)$ the probability that a bubble next to an $m$-sided bubble has $n$ sides. We present Glazier *et al.*'s results in Fig. 48 for the soap froth and the Potts model starting with identical initial conditions. As expected we find that few-sided bubble tend to be near many-sided bubbles. The converse does not hold, however. Six-sided bubbles like to cluster together, and seven-sided bubbles attract six-sided bubbles. Even more surprising, the distribution of neighbors of eight-sided bubbles is essentially the total distribution. Discounting the bias towards many- and few-sided bubbles that we have noted in the Potts model, the behavior of the distributions as a function of $m$ is identical for the model and the froth. Of the remaining models for which data are available, only the vertex model of Nakashima *et al.* comes close to reproducing the soap bubble correlation.